

## ORIGINAL ARTICLE

# Disease Systems Analysis of Bone Mineral Density and Bone Turnover Markers in Response to Alendronate, Placebo, and Washout in Postmenopausal Women

J Berkhout<sup>1,2,3\*</sup>, JA Stone<sup>4</sup>, KM Verhamme<sup>1</sup>, M Danhof<sup>2,3</sup> and TM Post<sup>2,3</sup>

A previously established mechanism-based disease systems model for osteoporosis that is based on a mathematically reduced version of a model describing the interactions between osteoclast (bone removing) and osteoblast (bone forming) cells in bone remodeling has been applied to clinical data from women ( $n = 1,379$ ) receiving different doses and treatment regimens of alendronate, placebo, and washout. The changes in the biomarkers, plasma bone-specific alkaline phosphatase activity (BSAP), urinary N-telopeptide (NTX), lumbar spine bone mineral density (BMD), and total hip BMD, were linked to the underlying mechanistic core of the model. The final model gave an accurate description of all four biomarkers for the different treatments. Simulations were used to visualize the dynamics of the underlying network and the natural disease progression upon alendronate treatment and discontinuation. These results complement the previous applications of this mechanism-based disease systems model to data from various treatments for osteoporosis.

*CPT Pharmacometrics Syst. Pharmacol.* (2016) 5, 656–664; doi:10.1002/psp4.12135; published online 21 November 2016.

## Study Highlights

### WHAT IS THE CURRENT KNOWLEDGE ON THE TOPIC?

☑ A mechanism-based model describing osteoblast and osteoclast activity was reduced in order to apply it in a population approach. Previously, it has been shown that the model reduction did not jeopardize the dynamical properties of the model. The reduced model was successfully applied to describe responses in different populations of postmenopausal women receiving different treatments (e.g., tibolone or calcium).

### WHAT QUESTION DID THIS STUDY ADDRESS?

☑ Is the current mechanism-based model able to accurately describe the disease progression in a new population receiving various doses and treatment regimens of alendronate? In other words, do the systems-related structure and parameter values that were fixed in this study allow for a description of a drug with a different mode of action than that was used before?

### WHAT THIS STUDY ADDS TO OUR KNOWLEDGE

☑ The model, with updated treatment functions, could describe the dynamics of two fast bone turnover markers (BSAP and NTX) and two slower markers (BMD at lumbar spine and total hip) from 1,379 study subjects divided over five different treatment arms to a very good approximation, showing the strength of a population systems pharmacology approach.

### HOW MIGHT THIS CHANGE DRUG DISCOVERY, DEVELOPMENT, AND/OR THERAPEUTICS?

☑ The results of this study allow for a better mechanistic understanding upon response to alendronate treatment and its washout. Additionally, these results complement the framework that is developed using this reduced mechanism-based model and provide a promising tool for the use of future applications of different treatments.

Mechanism-based models are based on underlying physiological networks. A fundamental property of a mechanism-based model is that it can be used under different circumstances than those in studies on which the model was developed (i.e., different drugs, different patients, etc.). An example for postmenopausal osteoporosis is the mechanism-based disease model developed by Lemaire *et al.*<sup>1</sup> Osteoporosis is a complex systemic skeletal disease resulting from an imbalance between bone resorption and bone formation. In women it is largely caused by a gradual loss of endogenous estrogen production during and following menopausal transition, which leads to an increased activity of osteoclast compared to

osteoblasts, a subsequent loss of bone, and eventually an increased fracture risk.<sup>2–5</sup>

The Lemaire model describes the interactions between osteoclast (bone removing) and osteoblast (bone forming) cells in bone remodeling. In its original form this model was not suitable to be applied in conjunction with advanced statistical techniques such as nonlinear mixed effects modeling (i.e., a population approach<sup>6</sup>). Therefore, Schmidt *et al.*, mathematically reduced the original model and, importantly, demonstrated that the model reduction did not jeopardize the model dynamics. Next, the reduced model was applied to clinical data from postmenopausal women receiving

<sup>1</sup>Department of Medical Informatics, Erasmus Medical Centre, Rotterdam, The Netherlands; <sup>2</sup>Leiden Academic Centre for Drug Research, Division of Pharmacology, Leiden, The Netherlands; <sup>3</sup>Leiden Experts on Advanced Pharmacokinetics and Pharmacodynamics (LAP&P), Leiden, The Netherlands; <sup>4</sup>Merck Sharp & Dohme Corp., Kenilworth, New Jersey, USA. \*Correspondence: J Berkhout ([jberkh@gmail.com](mailto:jberkh@gmail.com))

Received 1 April 2016; accepted 8 September 2016; published online on 21 November 2016. doi:10.1002/psp4.12135

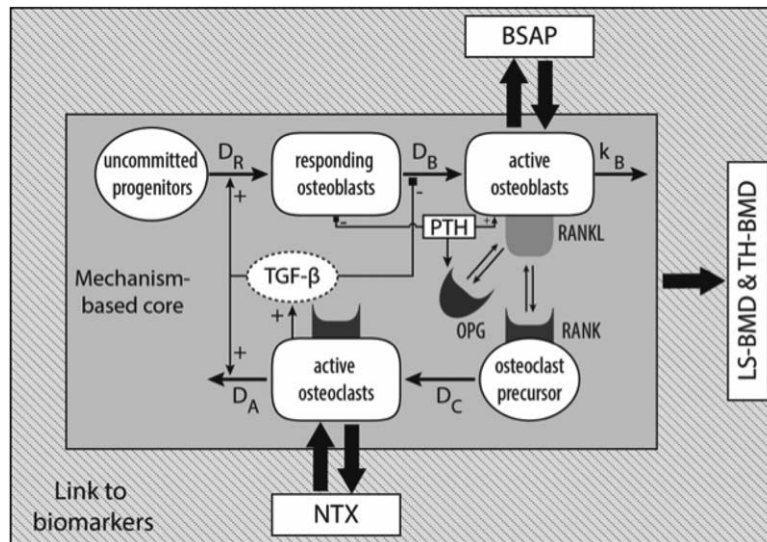


**Figure 1** Schematic representation of the mechanism-based disease systems analysis model. Active osteoblast and osteoclast cells and the indicated interactions form the mechanism-based core (shown in gray) of this model, which are linked to the biomarkers, NTX, BSAP, LS-BMD, and TH-BMD as shown in the striped area. PTH, parathyroid hormone, TGF- $\beta$ , transforming growth factor- $\beta$ , OPG, osteoprotegerin, RANK, receptor activator of NF- $\kappa$ B, RANKL, receptor activator of NF- $\kappa$ B ligand,  $D_R$  and  $D_B$  represent the differentiation rate of osteoblast progenitors and of responding osteoblasts, respectively,  $k_B$  is the apoptosis rate of active osteoblasts,  $D_C$  is the differentiation rate of osteoclast precursors, and  $D_A$  is the osteoclast apoptosis rate due to TGF- $\beta$ . RANKL binds to RANK and promotes osteoclast differentiation, while OPG inhibits this differentiation by binding RANKL. Upon differentiation, responding osteoblasts mature to active osteoblasts, which, in turn, are responsible for bone formation. Figure adapted from Ref. 8.

various doses of tibolone by Post *et al.*<sup>7</sup> Recently, the reduced model was applied to yet another clinical study population to describe the time course of osteoporosis in postmenopausal women receiving placebo.<sup>8</sup>

As there are usually no direct measures for the functioning of osteoblasts and osteoclasts available in clinical settings, different short-term biomarkers are used as indirect measures of their dynamics. Biomarkers for the activity of osteoblasts and osteoclasts are plasma bone-specific alkaline phosphatase (BSAP) and urinary N-telopeptide (NTX). Additionally, bone mineral density (BMD) in lumbar spine (LS) and total hip (TH) are primary clinical long-term biomarkers in the model. When the changes in these markers are linked to the underlying mechanism-based core of the model (**Figure 1**), these markers provide information about the different stages of the bone remodeling process, its dynamics, as well as the impact of therapeutic interventions on the progression of this disease.

In this study we applied the previously established reduced mechanism-based disease model to clinical data from postmenopausal women ( $n = 1,379$ ) receiving: 1) 2.5 or 5 mg of alendronate for 4 years, 2) placebo, or 3) 2 years of 2.5 or 5 mg alendronate followed by 2 years of placebo. Alendronate is a representative of the bisphosphonates, which are potent antiresorptive agents. After administration, alendronate binds to the bone mineral and is then taken up by osteoclasts where it inhibits enzymes in the cholesterol biosynthesis pathway, resulting, among other things, in apoptosis.<sup>9</sup> As alendronate is incorporated into bone, upon treatment discontinuation the bone surface is still less prone to breakdown, which can result in an ongoing slower breakdown of bone. Furthermore, alendronate

released by breakdown of alendronate-containing bone may be distributed to resorption surfaces that were not previously exposed to the drug, where it will inhibit resorption in proportion to its surface concentration. The doses and duration of alendronate treatment are relatively low and short (respectively), so the long-term posttreatment effects due to recycling of alendronate in bone are probably minimal in Early Postmenopausal Intervention Cohort (EPIC). So as a practical point, resolution of effect in EPIC is due mainly to drug on bone surfaces at the end of 2 years of treatment. We use the model to describe the changes in BMD and bone turnover markers in response to these various treatments. By doing so we will obtain deeper insight in the important dynamics involved in the disease progression and the underlying changes of the system during onset and offset of the alendronate treatment.

## METHODS

### Subject population and study design

Data were obtained from the EPIC study. This study was designed to study the efficacy and safety of daily oral alendronate treatment for prevention of postmenopausal osteoporosis. EPIC compared various regimens involving alendronate in doses of 2.5 or 5.0 mg per day with estrogen and with placebo. The study involved 1,609 postmenopausal women who were—after a 2-week, single-blind, placebo run-in period—randomly assigned in a double-blind manner to receive alendronate (Merck & Co., Whitehouse Station, NJ), placebo, or open-label estrogen-progestin. The total study duration was 4 years. In the current analysis, data from the subjects receiving treatment with

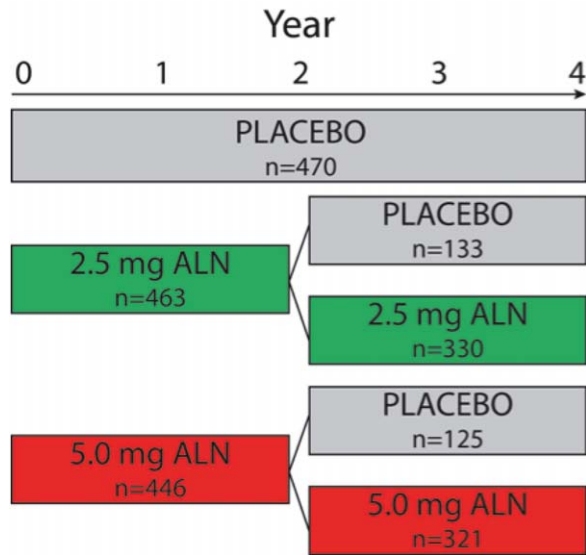


**Figure 2** Treatment allocation and sample size by treatment group and study year. Women were randomized to receive placebo, 2.5 or 5.0 mg alendronate once daily and numbers enrolled are shown for each treatment group. Women in the alendronate groups received alendronate during the first 2 years of the study. Treatment was then continued without change or was discontinued and replaced with placebo for the last 2 years of the study. ALN, alendronate.

estrogen were not included. Women in the alendronate groups received alendronate during the first 2 years of the study. Treatment was then continued without change or was discontinued and replaced with placebo for the last 2 years of the study (**Figure 2**). At baseline all participants were between 45 and 59 years of age, at least 6 months past menopause, in good general health, and had no clinical or laboratory evidence of confounding systemic disease. Four study centers (two in the US: Portland, Oregon, and Honolulu, Hawaii; and two in Europe: Nottingham, UK, and Copenhagen, Denmark) were involved in this trial. To ensure that most women who entered the study did not yet have osteoporosis, only 10% of the women enrolled at each center were allowed to have a baseline BMD at the spine (L1–L4) below 0.8 g/cm<sup>2</sup>, as measured by dual-energy x-ray absorptiometry. All women adhered to therapy (had taken at least 80% of the prescribed number of tablets, confirmed by tablet count). Dietary calcium intake was estimated at baseline and annually during the study on the basis of a food-frequency questionnaire. Further details about this study have been published elsewhere.<sup>8,10,11</sup>

#### Measurement of bone mineral density and biochemical markers of bone turnover

BMD of lumbar spine (LS) and total hip (TH) (defined as the femoral neck plus trochanter and intertrochanteric area) was measured by dual-energy x-ray absorptiometry (model 2000, Hologic, Waltham, MA) twice at baseline and annually thereafter. Blood and morning second-void urine samples were collected after an overnight fast at baseline and every 6 months thereafter. Bone resorption was estimated using urine N-telopeptide crosslinks of type I collagen (NTX)

(Osteomark, Ostex, Seattle, WA) as a biomarker. NTX is reported as nmol bone collagen equivalents (bce) and corrected for creatinine excretion (nmol bce/mmol cr). Serum level of bone-specific alkaline phosphatase (BSAP) was measured at baseline and at months 6, 12, 24, 36, 42, and 48 in a random sample of 550 women to estimate bone formation (Ostase, Hybritech, San Diego, CA). BSAP is reported in ng/mL.

#### Mechanism-based disease systems analysis model

For a detailed description of the model, see Ref. 8. The mechanism-based core of this model is governed by the following equations that take osteoblast activity ( $B$ ) relative to its baseline activity,  $B_0$  ( $y = B/B_0$ ) and the osteoclast ( $C$ ) activity relative to its baseline activity,  $C_0$  ( $z = C/C_0$ ):

$$\begin{cases} \frac{dy}{dt} = k_B \{ \sigma(z) - y \} \\ \frac{dz}{dt} = D_A \frac{1}{1+z^s} \left\{ \frac{1+b}{1+bf(t)\sigma^2(z)} y \cdot P_{Ca} - \sigma(z)z \cdot E_{ALN} \right\} \end{cases} \quad (1a)$$

$$\sigma(z) = (1+z^s) \frac{z}{z+z^s}, \quad z^s = \frac{C^s}{C_0} \quad (1b)$$

$$f(t) = e^{-k_{estrogen} t} \quad (1c)$$

In this equation  $f(t)$ ,  $P_{Ca}$ ,  $E_{ALN}$  represent disease progression, placebo, and alendronate treatment functions, respectively. In Eq. 1a the following system-specific parameters can be identified:  $z^s$ , a constant in  $\sigma(z)$  defined as  $C^s/C_0$  ( $C^s$  is the value of  $C$  for which approximately half of the transforming growth factor beta (TGF- $\beta$ ) receptors are occupied<sup>1</sup>);  $k_B$  is the elimination rate constant of osteoblast;  $k_{estrogen}$  is the estrogen elimination rate constant;  $D_A$  is the osteoclast apoptosis rate constant and  $b$  is the status of the disease at baseline. All subjects received treatment with placebo, whereas alendronate was only received by subjects in the alendronate treatment arms. Both treatments started at the same time ( $t_{start}$ ) and the effect of placebo was extensively discussed and described previously<sup>8</sup>:

$$P_{Ca}(t) = \begin{cases} 1 & \text{for } 0 < t < t_{start} \\ 1 - P_{max} (1 - e^{-k_{Ca,onset}(t-t_{start})}) \cdot e^{-k_{Ca,offset}(t-t_{start})} & \text{for } t > t_{start} \end{cases} \quad (2)$$

where  $P_{max}$  is a measure for the calcium induced inhibition of the RANK- RANKL-OPG through parathyroid hormone (PTH).<sup>1,12,13</sup> Treatment effects of alendronate could either be due to stimulation of apoptosis of active osteoclast or by inhibition of osteoclast activity.<sup>14</sup> In the model alendronate increases the apparent apoptosis of osteoclasts due to direct stimulation of apoptosis:

$$E_{ALN}(t) = I_{max, ALN} \frac{ALN}{ID_{50} + ALN} \quad (3a)$$

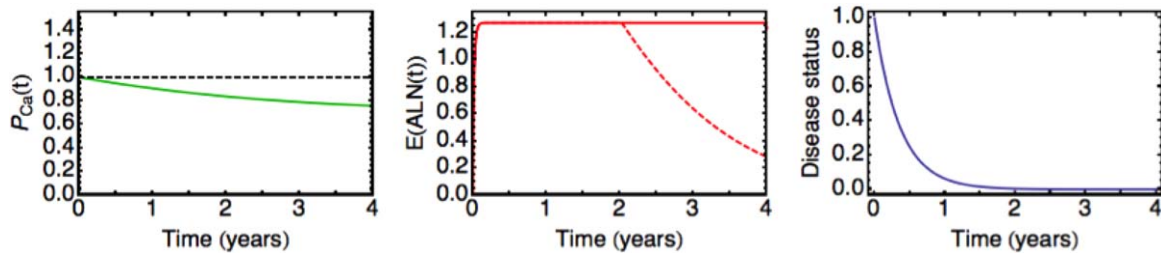


**Figure 3** Treatment functions used in the model. For the duration of the clinical study of 4 years the placebo function is shown in the left panel. The alendronate treatment function is shown in the middle panel for the subjects who continued with active treatment (solid line) and for the switchers to placebo (dashed line). The right panel shows the disease progression function, in which 1 represents a healthy status and 0 full disease.

$$ALN(t) = ALN_{\max} \times \begin{cases} 0 & \text{for } 0 < t < t_{\text{start}} \\ 1 - e^{-k_{\text{drugon}}(t - t_{\text{start}})} & \text{for } t_{\text{start}} < t < t_{\text{end}} \\ (1 - e^{-k_{\text{drugoff}}(t_{\text{end}} - t_{\text{start}})}) \cdot e^{-k_{\text{drugoff}}(t - t_{\text{end}})} & \text{for } t_{\text{end}} < t < \infty \end{cases} \quad (3b)$$

The factor  $I_{\max,ALN}$  represents the maximum treatment effect of alendronate and  $ID_{50}$  is the dose at which its half-maximum effect is reached.  $k_{\text{drugon}}$  and  $k_{\text{drugoff}}$  are the rate constants for onset and elimination of alendronate for the effects on the core system.

The panels in **Figure 3** show an illustration of the dynamics of the placebo, alendronate treatment and disease progression function.

The link to the biomarkers is achieved using the following equations:

$$\frac{dBSAP}{dt} = BSAP_0 \cdot (1 + \lambda_{BSAP,0}) \cdot y^{\rho_{BSAP}} \quad (4a)$$

$$\frac{dNTX}{dt} = NTX_0 \cdot z^{\rho_{NTX}} \quad (4b)$$

$$\frac{dLS-BMD}{dt} = kin_{LS} \cdot y^{\rho_B} - kout_{LS} \cdot z^{\rho_C} \cdot LS-BMD \quad (4c)$$

$$\frac{dTH-BMD}{dt} = kin_{TH} \cdot y^{\rho_B} - kout_{TH} \cdot z^{\rho_C} \cdot TH-BMD \quad (4d)$$

where “0” indicates baseline value.  $\lambda_{BSAP,0}$  is a scaling parameter to account for different units of BSAP reported in different clinical studies.<sup>8</sup>  $\rho$  is a positive transduction parameter, which links relative changes in cell activity to those in the corresponding bone turnover markers:  $\rho_{BSAP}$  and  $\rho_{NTX}$  for BSAP and NTX, respectively, and  $\rho_B$  and  $\rho_C$  for relative osteoblast and osteoclast activity, respectively.  $kin_{LS(TH)}$  is a zero-order production rate constant for LS-BMD (TH-BMD),  $kout_{LS(TH)}$  is the first-order degradation rate constant for LS-BMD (TH-BMD).

Body composition is known to induce changes in bone morphology.<sup>15</sup> Body mass index (BMI) was incorporated as a fraction of  $LS-BMD_0$  and  $TH-BMD_0$  using the median BMI of 25.4 kg/m<sup>2</sup>.

In order to initialize the model at a healthy normal state ( $z, y, \text{ and } S = 1$ ) individual time scales were normalized using time-since-onset-of-menopause as the characteristic time frame (see also Figure 2 in Ref. 8).

### Data analysis

R<sup>16</sup> was used for data management and plotting. The model was implemented in NONMEM, V7.3 (ICON Development Solutions, Ellicott City, MD), using ADVAN-6 and FOCE-I. Visual predictive check (VPC), using 500 simulations, were generated using PsN.<sup>17</sup> Pirana<sup>18</sup> and Xpose<sup>19</sup> were used for model management and for plotting and analyzing NONMEM output, respectively. Simulations of the final model were performed with Mathematica V9.0.

Prior to all analysis, measures for bone turnover markers and BMD were log-transformed. The variance of random interindividual variability on parameters was modeled by an exponential model:

$$P_i = P_p \cdot e^{\eta^i} \quad (5)$$

where  $P_p$  is the population value for parameter  $P$ ,  $P_i$  the value for this parameter for the  $i$ th individual, and  $\eta^i$  is the interindividual random deviation, which is assumed to be normally distributed with mean 0 and variance  $\omega^2$ . The residual variability resulting from measurement error and model misspecification was parameterized as standard deviation. The difference between observed and individual predicted concentrations was modeled as an additive error on logarithmic transformed data by:

$$\ln(y_{\text{obs}}) = \ln(y_{\text{pred}}) + \varepsilon_{ij} \quad (6)$$

where  $\varepsilon_{ij}$  is the residual error, with mean 0 and variance  $\sigma^2$ , between the  $j$ th observation in the  $i$ th individual  $\ln(y_{\text{obs}})$  and its prediction  $\ln(y_{\text{pred}})$ .

A considerable amount of between-subject variability was found for the baseline values of NTX and BSAP, possibly indicating issues with fasting, measurement precision, or biological variation.<sup>13</sup> Therefore, a second residual variability term  $\varepsilon_{ij2}$  was included to account for extreme bone turnover measures, those below the 1% and above the 99% quantile of the population distribution of the respective marker:

$$\ln(y_{\text{obs}}) + \varepsilon_{ij1} + W \cdot \varepsilon_{ij2} \quad (7)$$

where  $W = 1$ , and  $W = 0$  for measures above the 1% and below the 99% quantile. This adjustment positively influenced stability and parameter identifiability of the model and allowed inclusion of all available data.

**Table 1** Baseline demographic characteristics of the different treatment arms from the EPIC study.

Characteristic	Placebo	2.5 mg	2.5 mg → placebo	5.0 mg	5.0 mg → placebo
Subjects, n	470	330	133	321	125
Mean age at baseline ± SD, years	53.3 ± 3.7	53.3 ± 3.6	53.7 ± 3.5	53.4 ± 3.5	53.7 ± 3.6
Mean BMI at baseline ± SD, kg/m <sup>2</sup>	25.2 ± 3.6	25.6 ± 3.6	25.3 ± 3.8	25.1 ± 3.7	26.2 ± 3.5
Mean time since menopause at baseline ± SD, years	5.7 ± 5.4	6.3 ± 5.9	6.3 ± 6.0	6.5 ± 5.9	6.1 ± 5.5
Mean LS-BMD at baseline ± SD, g/cm <sup>2</sup>	0.94 ± 0.12	0.93 ± 0.12	0.94 ± 0.14	0.95 ± 0.13	0.96 ± 0.14
Mean TH-BMD at baseline ± SD, g/cm <sup>2</sup>	0.85 ± 0.11	0.84 ± 0.11	0.83 ± 0.12	0.85 ± 0.12	0.86 ± 0.11
Mean BSAP at baseline ± SD (ng/ml)	11.2 ± 4.4	10.9 ± 3.9	10.1 ± 3.7	10.9 ± 3.7	10.8 ± 4.2
Mean NTX at baseline ± SD, nmol bce/mmol cr	88.0 ± 45.0	83.3 ± 46.4	83.6 ± 41.7	86.0 ± 48.2	86.6 ± 47.2

Throughout model development diagnostic and individual plots were inspected and used together with the drop in objective function to come to the final model.

## RESULTS

Of the 1,609 women enrolled in the EPIC study,<sup>10</sup> data from 1,379 were used in this study (i.e., excluding estrogen treatment group). Of these study subjects, the baseline demographic characteristics, years since menopause, LS-BMD, TH-BMD, BSAP, and NTX are shown in **Table 1**. There were no significant differences between the treatment groups at baseline.

### Final disease systems analysis model

The changes in LS-BMD and TH-BMD were best described using a nonlinear indirect response model (Eq. 4c,d), as previously described by others.<sup>20,21</sup> The mechanism of action of alendronate was included as an induction of the elimination of osteoclasts cells and reflects the interference of alendronate with the osteoclast functioning. Whether this is through increased apoptosis or just a permanent dysfunction state being created by alendronate cannot be ruled out from our data. This parameterization was chosen upon inspection of the mechanism of action and the time course profiles of the bone turnover marker as presented by Greenspan *et al.*<sup>22</sup> The parameter estimates and interindividual variability (IIV) of the final model are presented in **Table 2**. All parameters in the final model could be estimated with a good precision (coefficient of variation well below 40%).

### Visual predictive check

To test whether the final model is able to describe the average trends and the variability in the observed data a visual predictive check (VPC) was performed. Plots split by treatment group for the markers NTX (degradation), BSAP (formation), LS-BMD, and TH-BMD (integrated markers), are presented in **Figure 4**. The model adequately describes the biomarker data at all dose levels as the 5th, 50th, and 95th percentiles of the real data (red lines) overlap with the 5th, 50th, and 95th percentiles of the simulated data (black lines) and lie within the respective prediction intervals of the simulations (blue and red areas). Furthermore, the 5th, 50th, and 95th percentiles of the model prediction (black lines) follow that of the real data (red lines).

Upon treatment with alendronate a sharp decrease in BSAP and NTX was observed, which remained low for the 4 years of treatment or returned towards the baseline values for treatment discontinuation. Note, however, that the levels

were not yet back at their baseline values after 4 years since the start of the study. Also interesting to note is the fact that the return of the biomarkers towards baseline values upon treatment discontinuation is slower than the onset after start of treatment. This could be the result of multiple phenomena occurring simultaneously: a return component that has similar kinetics as onset, but that only partially returns one to baseline and a remaining return that is much slower, likely influenced by the slow washout of the drug incorporated into bone. Bisphosphonate within bone is inactive and the pharmacologic activity is driven by the drug that is released from the long-term bone depot through ongoing bone remodeling.

Furthermore, it can be seen that the onset of the effect on NTX is more rapid than for BSAP. This difference leads to the creation of a window, where the effect on bone formation lags behind that of bone resorption. The effect of this window is observed in the LS-BMD and TH-BMD dynamics, where during placebo treatment there is a decrease in BMD, while during treatment with alendronate an increase in BMD is observed that is proportional with dose. During years 3 and 4, for BMD a decrease in LS and TH is observed in participants who switched from alendronate to placebo.

Overall, the VPC plots give an impression of the ability of the disease system approach to provide a physiological framework extracting the information available in multiple markers, which operate on different timescales.

### Simulations

In order to obtain deeper insight into the underlying model dynamics responsible for the observed alendronate response, simulations with the final model were performed. Simulations were performed with the population parameters, as shown in **Table 2**. We see (**Figure 5**) that upon treatment with alendronate (solid lines) a sharp decline in osteoclast activity followed by a decline in osteoblast activity. When treatment is discontinued after 2 years (dashed lines), the activities of both cell types increase again. When only placebo is given, an increase in activities of both cells is observed (dotted lines). Changes in BMD are determined by the relative activities of osteoclast and osteoblast cells. To visualize this, a variable  $S = z/y$  was introduced. Thus, when  $S$  is smaller than 1 (green area), osteoblasts activity ( $y$ ) is bigger than osteoclast ( $z$ ), and hence BMD will increase. For all panels solid lines correspond to treatment with 5 mg of alendronate, dotted lines to placebo, and the dashed lines show the treatment arm that received 5 mg alendronate for the first 2 years followed by 2 years of placebo.

**Table 2** Population parameter estimates of the final model.

Parameter (unit)	Description	Value (%CV)
<b>System related parameters</b>		
$z_s$ (fraction)	Constant in $\sigma(z)$	0.659 (fixed)
$k_B$ ( $\text{day}^{-1}$ )	Elimination rate constant of osteoblast	0.0109 (fixed)
$k_{\text{estrogen}}$ ( $\text{day}^{-1}$ )	Estrogen elimination rate constant	0.00763 (fixed)
$D_A$ ( $\text{day}^{-1}$ )	Osteoclast apoptosis rate constant	1 (fixed)
$b$ (%)	Status of the disease process at baseline	1 (fixed)
<b>Placebo related parameters</b>		
$k_{\text{Ca,onset}}$ ( $\text{day}^{-1}$ )	Calcium elimination rate constant for onset	0.000304 (8.6)
$k_{\text{Ca,offset}}$ ( $\text{day}^{-1}$ )	Calcium elimination rate constant for offset	0.000269 (16.9)
<b>Treatment related parameters</b>		
$I_{\text{max,ALN}}$ (-)	Maximum alendronate effect	0.841 (3.6)
$\text{ALN}_{\text{max}}$ (mg)	Maximum alendronate exposure	5.0 (fixed)
$\text{ID}_{50}$ (mg)	The dose at which its half-maximum effect is reached	6.05 (38.5)
$k_{\text{drugon}}$ ( $\text{day}^{-1}$ )	Alendronate onset rate constant	0.132 (35.6)
$k_{\text{drugoff}}$ ( $\text{day}^{-1}$ )	Alendronate elimination rate constant	0.0285 (21.2)
<b>Transducer function bone turnover markers</b>		
$\text{BSAP}_0$ (U/L)	BSAP baseline value	97.4 (fixed)
$\lambda_{\text{BSAP}0}$ (-)	BSAP baseline scaling parameter	-0.92 (0.2)
$\text{NTX}_0$ (nmol bce/mmol cr)	NTX baseline value	30.0 (4.2)
$\rho_{\text{BSAP}}$ (-)	BSAP transduction parameter	1.45 (7.4)
$\rho_{\text{NTX}}$ (-)	NTX transduction parameter	1.22 (6.0)
<b>Transducer function bone mineral density</b>		
$k_{\text{in,ls}}$ (mg/day)	Zero-order production rate constant for LS-BMD	0.212 (11.2)
LS-BMD <sub>0</sub> ( $\text{g}/\text{cm}^2$ )	LS-BMD baseline value	1.02 (0.5)
BMI-LS-BMD <sub>0</sub> fraction (-)	BMI fraction of LS-BMD baseline	0.0102 (9.6)
$k_{\text{in,th}}$ (mg/day)	Zero-order production rate constant for TH-BMD	0.139 (11.4)
TH-BMD <sub>0</sub> ( $\text{g}/\text{cm}^2$ )	TH-BMD baseline value	0.91 (0.5)
BMI-TH-BMD <sub>0</sub> fraction (-)	BMI fraction of TH-BMD baseline	0.0164 (6.0)
$\rho_B$ (-)	Osteoblast transduction parameter	1.67 (16.3)
$\rho_C$ (-)	Osteoclast transduction parameter	0.784 (12.6)
<b>Inter individual variability</b>		
IIV $\text{NTX}_0$ (%)	IVV NTX baseline	36.2 (2.6)
IIV $\text{BSAP}_0$ (%)	IVV BSAP baseline	28.9 (3.7)
corr $\text{NTX}_0$ - $\text{BSAP}_0$ (-)	IVV correlation NTX-BSAP baseline	0.47 (10.4)
IIV $\text{BMD}_{\text{LS},0}$ (%)	IVV LS-BMD baseline	12.5 (2.1)
IIV $\text{BMD}_{\text{TH},0}$ (%)	IVV TH-BMD baseline	12.2 (1.9)
corr $\text{BMD}_{\text{LS},0}$ - $\text{BMD}_{\text{TH},0}$ (-)	IVV correlation LS-TH-BMD baseline	0.65 (1.5)
<b>Residual variability</b>		
$\epsilon_{\text{BSAP}}$ (SD)	Residual variability BSAP	0.185 (2.7)
$\epsilon_{\text{BSAP,extremes}}$ (SD)	Residual variability BSAP extremes	0.505 (10.1)
$\epsilon_{\text{NTX}}$ (SD)	Residual variability NTX	0.321 (1.1)
$\epsilon_{\text{NTX, extremes}}$ (SD)	Residual variability NTX extremes	0.281 (7.2)
$\epsilon_{\text{LS}}$ (SD)	Residual variability LS-BMD	0.024 (1.5)
$\epsilon_{\text{TH}}$ (SD)	Residual variability LS-BMD	0.019 (1.4)

For the bone turnover markers, we observe a sharp and rapid decrease in NTX (degradation marker) and slower decrease in BSAP (formation marker). This results in an increase in BMD at the lumbar spine (green) and total hip (brown) that is around 2–3% compared to the baseline value. Please note that EPIC was intended as an osteoporosis prevention trial; beyond the modest increase in BMD seen with alendronate treatment, the drug is preventing further loss in BMD as seen with only placebo treatment. Interestingly, this difference in onset was also observed in the

description of the VPC results. An advantage of simulations is a continuous response, whereas in the available clinical data the first measurement after treatment was only after 6 (NTX) or 12 months (BSAP). From the simulations it was observed that NTX is at its lowest value within 1 month, whereas the minimal level of BSAP is obtained around 6 months. This compares to previously published data where NTX reaches its maximum within 2 to 4 weeks.<sup>23</sup>

When treatment is switched to placebo after 2 years, the activity of osteoblast, osteoclast, and levels of NTX and BSAP



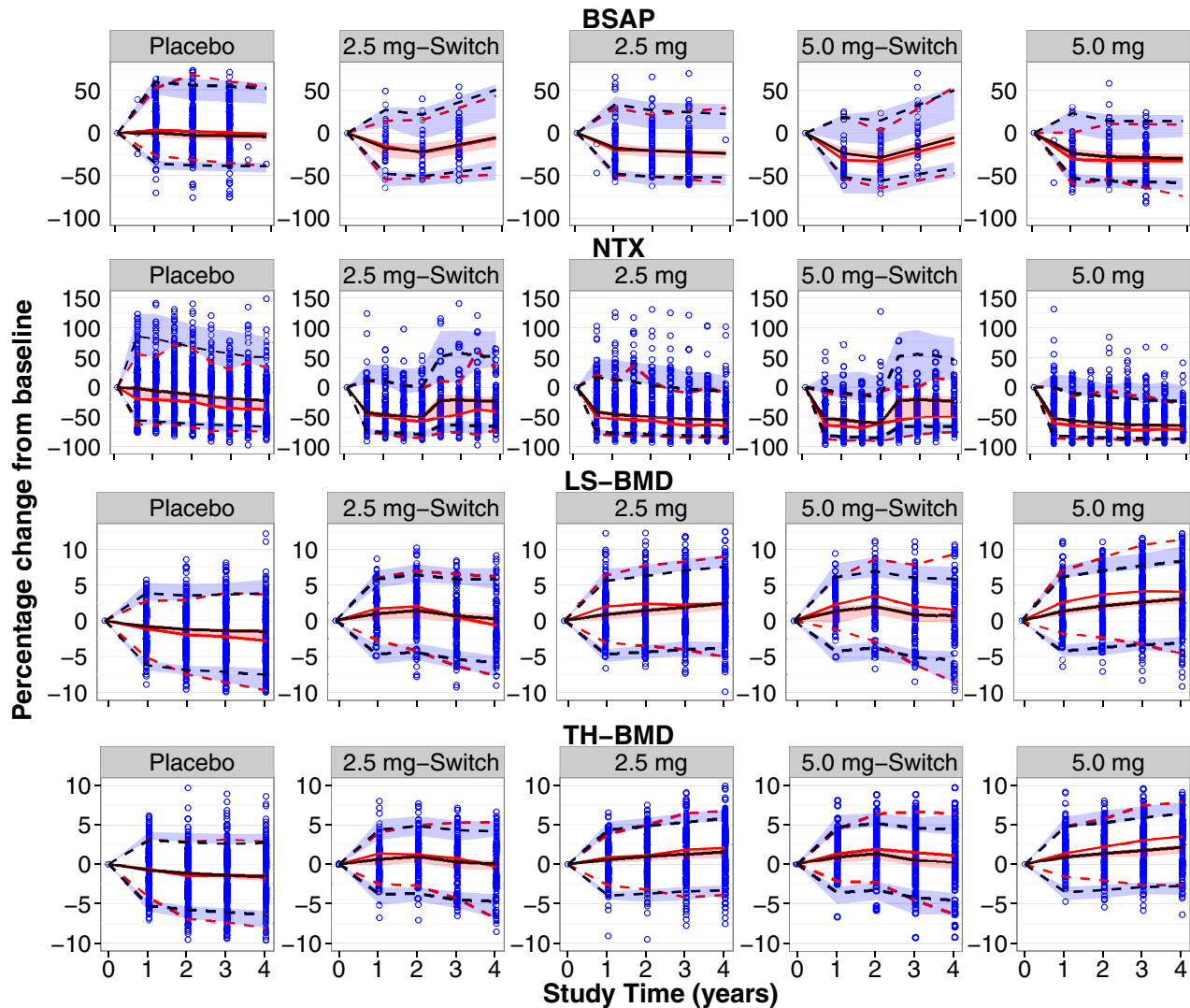


**Figure 4** Visual predictive check (VPC) plots. The columns show the different treatment groups, from left to right: placebo, 2 years 2.5 mg alendronate followed by 2 years placebo, 2.5 mg alendronate, 2 years 5.0 mg alendronate followed by 2 years placebo, 5.0 mg alendronate. The rows correspond to the different markers, from top to bottom: the bone formation marker BSAP, the degradation marker NTX, LS-BMD and TH-BMD. All markers are plotted as a percentage change relative to baseline vs. the study time scale. The blue dots represent the percentage change from baseline of the available observations. The 5th, 50th, and 95th percentiles of the real data in the bins are presented by the red dashed, red solid, and red dashed line, respectively. The 5th, 50th, and 95th percentiles of the simulated data ( $n = 500$ ) in the bins are presented by the black dashed, black solid, and black dashed line, respectively. The confidence interval for the simulated data 5th, 50th, and 95th percentiles for each of the bins is presented by the blue, red, and blue area, respectively.

change in the direction of their pretreatment values, leading to a decrease in BMD. This decrease is smaller compared to the subjects receiving placebo treatment for 4 years. Four years of treatment with placebo results in a continuous decline in BMD that is on the order of 1–2% below their baseline value.<sup>10</sup>

## DISCUSSION

In this study we applied a mechanism-based disease systems analysis to clinical trial data from postmenopausal women who were treated with various doses of alendronate, placebo, or a combination of active treatment followed by placebo. In line with results from earlier studies, 4 years of

alendronate treatment prevented postmenopausal bone loss at the lumbar spine and total hip and was more effective than 2 years of alendronate treatment followed by 2 years of placebo. In addition, increased BMD at these two sites was maintained in women who received alendronate for 4 years.<sup>10,11,24</sup> The advantage of the mechanism-based model is that these observations can be linked to the underlying changes in activities of osteoblast and osteoclast cells. The simulations support that NTX and BSAP closely follow the dynamics of osteoclasts and osteoblasts, and their combined activity,  $S = z/y$ , determines changes in BMD through the nonlinear indirect response model of Eq. (4c,d). Since the ratio  $S$  drops well below unity for a longer period of time during treatment, BMD increases.

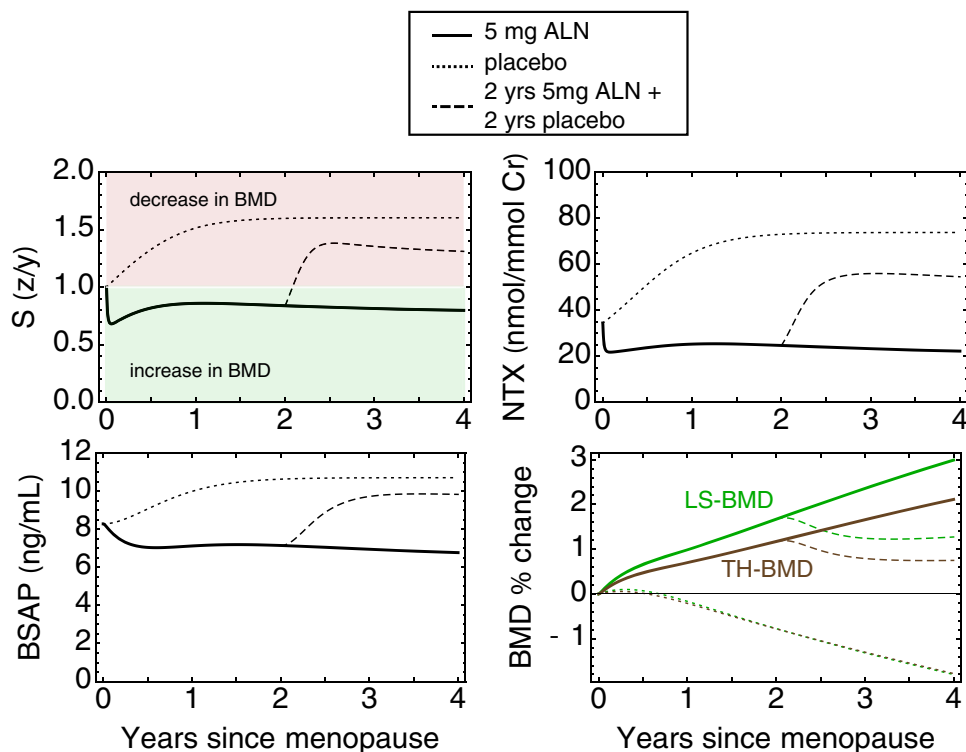


**Figure 5** Model simulations. In the upper left panel the relative activity of osteoblast ( $y$ ) and osteoclast ( $z$ ) is shown as the ratio  $S = z/y$ . For  $S < 1$ , there is an increase in BMD as indicated by the green area, when  $S > 1$ , BMD decreases (red area). The upper right and lower left panels show the dynamics of the bone markers NTX and BSAP, respectively. The lower right panel shows the change in LS-BMD (green) and TH-BMD (brown) as percentage change from baseline. In all plots dotted lines correspond to placebo treatment, solid lines to 4 years treatment of 5.0 mg of alendronate (ALN), and dashed lines to 2 years of alendronate treatment followed by 2 years of placebo treatment.

Our simulations further suggest that 4 years of treatment with alendronate had a disease-modifying (i.e., affecting the disease progression rate) effect on BMD. While the increase in BMD after 2 years of alendronate treatment decreases when treatment was switched to placebo for the last 2 years of the study, it did not decrease completely to baseline levels at year 4. This suggests a residual effect of previous treatment with alendronate, which may be caused in part because alendronate is retained in the skeleton. Also, alendronate had a symptomatic effect<sup>25</sup> on the bone turnover markers, since these levels almost return to their pretreatment levels (Figures 4 and 5), with the residual effect of incorporation of alendronate into the bone still visible. Furthermore, our analysis indicates that changes in BMD in total hip are slower ( $k_{in,th} = 0.139$  mg/day) than those in lumbar spine ( $k_{in,ls} = 0.212$  mg/day). These findings are in line with the underlying bone physiology as trabecular bone, which turns over faster than cortical bone, is present in larger quantities in the spine compared to the hip.

We were able to estimate all parameters with good precision (all coefficients of variation (CV)  $< 38.5\%$ ). However, for complex mathematical models caution should be taken with interpretation of these precision measures. For our model this was observed for the estimated value for the  $ID_{50}$  estimate for alendronate (6.05 mg). Despite a low CV, this estimate falls above the dose range (2.5–5 mg) available in the dataset. Preconditioning methods, as recently proposed,<sup>26</sup> can be informative for such identifiability

issues. Dose-ranging studies of alendronate for treatment of osteoporosis identified a similar response at 10 and 20 mg daily,<sup>27</sup> suggesting that the estimate from this analysis may be high. This could be due to limitations in the available dataset as well as potentially complexities in the dynamics of washout and switch to placebo treatment.

In comparison to the BMD equation that was used previously,<sup>8</sup> we obtained the best description of this dataset when a nonlinear BMD equation was used (Eq. 4c,d). This is also in line with results from others.<sup>21</sup> The nonlinear response in BMD is best visible from our model simulations. Whether the changes in BMD in this study population are truly nonlinear cannot be determined with the 1-year measurement frequency over this 4-year period.

This model has recently been applied to postmenopausal women receiving various doses of tibolone.<sup>7</sup> The mechanistic nature of this population model makes it possible to evaluate the effect of other drugs with different mechanisms and modes of action such as alendronate. This also shows the strength of a disease systems analysis<sup>25</sup> model; the core remains the same and the markers that supply the required information on the system can differ or come from different treatments, which is in contrast to empirical models where (single) marker(s) are directly linked. On the other side of the model spectrum, systems pharmacology models, integrate different signaling networks and organs to describe calcium homeostasis and bone remodeling.<sup>12,21</sup> Recently, such a systems pharmacology model was used



by the US Food and Drug Administration to evaluate the appropriateness of a proposed dosing regimen for a new biologic.<sup>28</sup> Due to their inherent complexity, the establishment of completely systems pharmacology models within a population framework is hindered by the inability to identify and estimate the pertinent model parameters.<sup>29</sup>

Despite the large number of subjects in this study and the crossover design, the initial dynamics of the systems could not be identified from these data. Probably this is due to the lack of data during the early treatment period. We anticipate, therefore, that with more data points available right after onset of treatment the system-specific parameter,  $D_a$ , i.e., osteoclast apoptosis rate constant, could be identifiable as well.

In conclusion, we applied a previously established mechanism-based model to a new set of clinical data from postmenopausal women receiving alendronate, placebo, or a combination of both (i.e., washout). We were able to identify the underlying changes in the bone remodeling network upon continuation and discontinuation of alendronate treatment. In addition, these results build upon the framework obtained with this mechanism-based model: first, it has been reduced,<sup>30</sup> followed by the application to different study populations receiving different treatments, including: tibolone,<sup>7</sup> placebo,<sup>8</sup> and now alendronate.

**Acknowledgments.** The authors thank Lambertus A. Peletier for insightful discussions on the model. Bruno Stricker and Miriam Sturkenboom are acknowledged for inspiring discussions. This study was performed within the framework of Dutch Top Institute Pharma, PKPD PLATFORM 2.0 (project number D2-501). This work was carried out on the Dutch national e-infrastructure with the support of SURF Foundation.

**Conflict of Interests.** The authors declare no conflicts of interest.

**Author Contributions.** J.B., J.A.S., K.M.V., M.D., and T.M.P. wrote the article; J.A.S., K.M.V., M.D., and T.M.P. designed the research; J.B. and T.M.P. performed the research; J.B., J.A.S., K.M.V., M.D., and T.M.P. analyzed the data.

1. Lemaire, V., Tobin, F.L., Greller, L.D., Cho, C.R. & Suva, L.J. Modeling the interactions between osteoblast and osteoclast activities in bone remodeling. *J. Theor. Biol.* **229**, 293–309 (2004).
2. Canalis, E., Giustina, A. & Bilezikian, J.P. Mechanisms of anabolic therapies for osteoporosis. *N. Engl. J. Med. Mass. Med. Soc.* **357**, 905–916 (2007).
3. Seeman, E. & Delmas, P.D. Bone quality—the material and structural basis of bone strength and fragility. *N. Engl. J. Med.* **354**, 2250–2261 (2006).
4. Poole, K.E.S. & Compston, J.E. Osteoporosis and its management. *BMJ* **333**, 1251–1256 (2006).
5. Salari Sharif, P., Abdollahi, M. & Larjani, B. Current, new and future treatments of osteoporosis. *Rheumatol. Int.* **31**, 289–300 (2011).
6. Lavielle, M. *Mixed Effects Models for the Population Approach: Models, Tasks, Methods and Tools* (Chapman and Hall/CRC, 2014).
7. Post, T.M. *et al.* Application of a mechanism-based disease systems model for osteoporosis to clinical data. *J. Pharmacokinet. Pharmacodyn.* **40**, 143–156 (2013).
8. Berkhout, J. *et al.* Application of a systems pharmacology-based placebo population model to analyze long-term data of postmenopausal osteoporosis. *CPT Pharmacometrics Syst. Pharmacol.* **4**, 516–526 (2015).
9. Fisher, J.E. *et al.* Alendronate mechanism of action: geranylgeraniol, an intermediate in the mevalonate pathway, prevents inhibition of osteoclast formation, bone resorption, and kinase activation in vitro. *Proc. Natl. Acad. Sci. U. S. A.* **96**, 133–138 (1999).
10. Ravn, P. *et al.* Alendronate and estrogen-progestin in the long-term prevention of bone loss: four-year results from the early postmenopausal intervention cohort study. A randomized, controlled trial. *Ann. Intern. Med.* **131**, 935–942 (1999).
11. Hosking, D. *et al.* Prevention of bone loss with alendronate in postmenopausal women under 60 years of age. *N. Engl. J. Med.* **338**, 485–492 (1998).
12. Peterson, M.C. & Riggs, M.M. A physiologically based mathematical model of integrated calcium homeostasis and bone remodeling. *Bone*. **46**, 49–63 (2010).
13. Post, T.M., Cremers, S.C.L.M., Kerbusch, T. & Danhof, M. Bone physiology, disease and treatment: towards disease system analysis in osteoporosis. *Clin. Pharmacokinet.* **49**, 89–118 (2010).
14. Fisher, J.E., Rosenberg, E., Santora, A.C. & Reszka, A.A. In vitro and in vivo responses to high and low doses of nitrogen-containing bisphosphonates suggest engagement of different mechanisms for inhibition of osteoclastic bone resorption. *Calcif. Tissue Int.* **92**, 531–538 (2013).
15. Orozco, P. & Nolla, J.M. Associations between body morphology and bone mineral density in premenopausal women. *Eur. J. Epidemiol.* **13**, 919–924 (1997).
16. R Core Team. R: A Language and Environment for Statistical Computing (Vienna, Austria, 2013).
17. Lindbom, L., Pihlgren, P., Jonsson, E.N. & Jonsson, N. PsN-Toolkit—a collection of computer intensive statistical methods for non-linear mixed effect modeling using NONMEM. *Comput. Methods Programs Biomed.* **79**, 241–257 (2005).
18. Keizer, R.J., van, Benten M., Beijnen, J.H., Schellens, J.H.M. & Huitema, A.D.R. Pirana and PCluster: a modeling environment and cluster infrastructure for NONMEM. *Comput. Methods Programs Biomed.* **101**, 72–79 (2011).
19. Jonsson, E.N. & Karlsson, M.O. Xpose—an S-PLUS based population pharmacokinetic/pharmacodynamic model building aid for NONMEM. *Comput. Methods Programs Biomed.* **58**, 51–64 (1999).
20. Marathe, D.D., Marathe, A. & Mager, D.E. Integrated model for denosumab and ibandronate pharmacodynamics in postmenopausal women. *Biopharm. Drug Dispos.* **481**, 471–481 (2011).
21. Peterson, M.C. & Riggs, M.M. Predicting nonlinear changes in bone mineral density over time using a multiscale systems pharmacology model. *CPT Pharmacometrics Syst. Pharmacol.* **1**, e14 (2012).
22. Greenspan, S.L. *et al.* Significant differential effects of alendronate, estrogen, or combination therapy on the rate of bone loss after discontinuation of treatment of postmenopausal osteoporosis. A randomized, placebo-controlled trial. *Ann. Intern. Med.* **137**, 875–883 (2002).
23. Greenspan, S.L., Resnick, N.M. & Parker R.A. Early changes in biochemical markers of bone turnover are associated with long-term changes in bone mineral density in elderly women on alendronate, hormone replacement therapy, or combination therapy: a three-year, double-blind, placebo-controlled, randomized clinical trial. *J. Clin. Endocrinol. Metab.* **90**, 2762–2767 (2005).
24. McClung, M.R. *et al.* Prevention of postmenopausal bone loss: six-year results from the Early Postmenopausal Intervention Cohort Study. *J. Clin. Endocrinol. Metab.* **89**, 4879–4885 (2004).
25. Post, T.M., Freijer, J.I., DeJongh, J. & Danhof, M. Disease system analysis: basic disease progression models in degenerative disease. *Pharm. Res.* **22**, 1038–1049 (2005).
26. Aoki, Y., Nordgren, R. & Hooker, A.C. Preconditioning of nonlinear mixed effects models for stabilisation of variance-covariance matrix computations. *AAPS J.* **18**, 505–518 (2016).
27. Liberman, A.U. Effect of oral alendronate on bone mineral density and the incidence of fractures in postmenopausal osteoporosis. *N. Engl. J. Med.* **333**, (1995).
28. Peterson, M.C. & Riggs, M.M. FDA advisory meeting clinical pharmacology review utilizes a quantitative systems pharmacology (QSP) Model: A watershed moment? (2014), 2–5 (2015).
29. Post, T.M. Disease system analysis between complexity and (over) simplification. Doctoral thesis, Leiden University (2009).
30. Schmidt, S., Post, T.M., Peletier, L.A., Boroujerdi, M.A. & Danhof, M. Coping with time scales in disease systems analysis: application to bone remodeling. *J. Pharmacokinet. Pharmacodyn.* **38**, 873–900 (2011).

© 2016 The Authors CPT: Pharmacometrics & Systems Pharmacology published by Wiley Periodicals, Inc. on behalf of American Society for Clinical Pharmacology and Therapeutics. This is an open access article under the terms of the Creative Commons Attribution-NonCommercial-NoDerivs License, which permits use and distribution in any medium, provided the original work is properly cited, the use is non-commercial and no modifications or adaptations are made.

Supplementary information accompanies this paper on the CPT: Pharmacometrics & Systems Pharmacology website (<http://www.wileyonlinelibrary.com/psp4>)